Shape Reconstruction of Post-Buckled Panels in a Wagner-Beam Test-Rig Using Distributed Optical Sensors and Digital Image Correlation

PIETRO ACETI, SEBASTIAN STAMMEL, GIUSEPPE SALA and CHIARA BISAGNI

ABSTRACT

This paper compares out-of-plane displacement measurement techniques between a digital image correlation system and a distributed optical fiber sensor system for shear-loaded panels in a Wagner beam. The digital image correlation system determines the displacement directly and the distributed optical fiber sensors use Ko's displacement theory for strain-based displacement calculation. In this study, the Wagner beam was shear-loaded and the panel strain was elastic and reversible. This paper shows that the digital image correlation system is state-of-the-art for determining the panel's out-of-plane displacement. The displacement estimation by the distributed optical fiber system requires a precise setup and an extension of Ko's displacement theory for this specific testing situation.

INTRODUCTION

Structural deformation monitoring plays a crucial role in the design, operation, and maintenance of future aerospace structures with the increasing use of composite materials and morphing structural elements. Strain monitoring improves the ability to detect damage in real-time, and therefore also the maintenance service and structural performance [1]. Shape detection also enables real-time evaluation of deformed structures and the implementation of a control system for the use of morphing structures [2].

There are multiple methods to measure the structural strain. One is the use of digital image correlation systems (DIC) to measure the shape [3]. The DIC system is based on an optical image method and shows the deformed shape directly. However, the DIC system requires equipment space and, therefore, is impractical for operational application

Pietro Aceti, Researcher. Department of Aerospace Science and Technology, Politecnico di Milano, Milano, Italy
Sebastian Stammel, PhD Student. Department of Aerospace Science and Technology, Politecnico di Milano, Milano, Italy
Giuseppe Sala, Full Professor, Department of Aerospace Science and Technology, Politecnico di Milano, Milano, Italy
Chiara Bisagni, Full Professor, Department of Aerospace Science and Technology, Politecnico di Milano, Milano, Italy

in aerospace flying structures. Recent research focused on distributed optical fiber sensors (DOFS) to measure the strain continuously in real-time. The DOFS determines the strain, which is used to compute the structural deformation [4]. This technique can be applied to aerospace flying structures by bonding optical fibers onto components made of lightweight aluminum alloys or by embedding them into composite materials.
Three methods are available to calculate the deformed shape based on the strain distribution:

- Ko's displacement theory [5]
- Modal method [6]
- Inverse finite element method [7]

Contrary to the modal and inverse finite element methods, Ko's displacement theory does not require prior extensive numerical calculations. Ko's displacement theory uses closed-form equations derived from the classical Bernoulli-Euler beam theory to reconstruct the structural deformation based on measured strains [8]. The closed-form equations only require knowledge of the structural geometrical features. To determine the full-field deformation of a plate using the theory, a plate is divided into narrow strips and each strip considered as a DOFS path achieves a full-field deformation. For large deformation, Ko's displacement theory has to be expanded to cover nonlinearity [9]. This expansion is proposed and validated using curved displacement transfer functions [10, 11].

In this paper, two measurement methods determine the out-of-plane displacement of shear-loaded panels in a Wagner beam under large deformation. The DIC measurement is compared with DOFS displacement calculation. The comparison will provide a basis to evaluate the compatibility of both methods for practical application in aerospace structures like a wing box. In the chapter *Experimental Setup* the measurement methods are explained and the test setup is presented. *Results* provides a discussion of the results.

EXPERIMENTAL SETUP

The experimental testing was conducted with a two-bay Wagner beam experiencing shear-loading at the Department of Aerospace Science and Technology. This beam can sustain a downward force up to 20 kN without plastic deformation. The force was introduced vertical and central on the beam and the beam was mounted on steel podiums on each side. The loading was carried out manually with a screw jack. Aluminum-Alloy *EN AW 6060* panels were chosen for the Wagner beam.

A load cell and a linear variable differential transformer (LVDT) measure at the beam's load introduction point the applied force and the resulting vertical displacement. The strain was measured by means of four back-to-back monoaxial electrical resistance strain gauges (SG). Those SG were installed in the panel's center next to and in the direction of the DOFS as shown in Figure 1.

One side of the Wagner beam panels was instrumented with DOFS, which were bonded directly onto the plate surface using an epoxy adhesive. The strain was monitored along the compressed diagonals of the beam, as well as along two additional

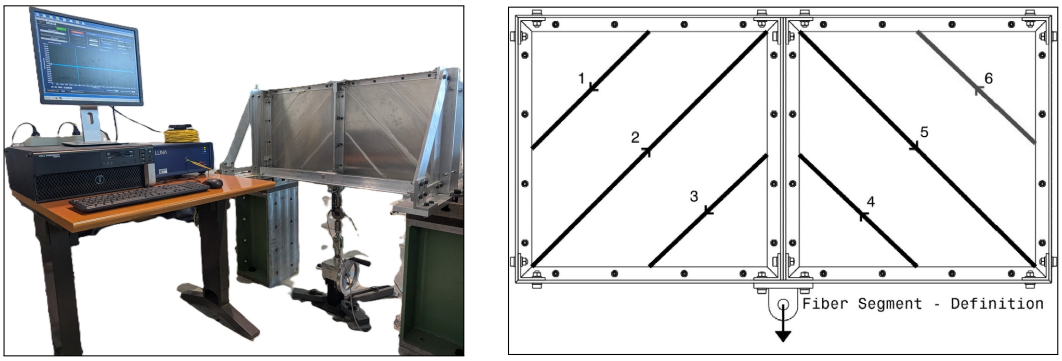

Figure 1. (Left) DOFS measurement system deployed on the Wagner Beam; (Right) Segment definition of the DOFS paths.

segments oriented parallel to the compressed diagonal, to enhance sensitivity to bending phenomena associated with buckling. In total, six measurement paths were defined, three on each plate. The DOFS was arranged accordingly to cover these six paths, as illustrated in Figure 1.

The DOFS enables strain measurement along its longitudinal axis. For this purpose, the ODiSI-B interrogator by Luna Innovations was employed. This device is a swept-wavelength interferometer capable of measuring Rayleigh backscatter within DOFS, which originates from random fluctuations in the refractive index along the fiber length. Variations in strain or temperature relative to a reference state result in a spectral shift of the backscattered light, which is quantified in equation 1.

$$\frac{\lambda - \lambda_0}{\lambda_0} = K_T(T - T_0) + K_\varepsilon(\varepsilon - \varepsilon_0) \tag{1}$$

$K_\varepsilon = 0.780$ and $K_T = 6.45 * 10^{-6}[1/^\circ C]$, strain and temperature sensitivity, are respectively used for the DOFS [12]. λ_0, T_0, and $\varepsilon_0 = 0$ are the wavelength, temperature, and strain at the initial reference state. The test involves loading and unloading of the Wagner beam, which lasts only a few seconds and therefore is assumed $T - T_0 = 0$ like in equation 2.

$$\varepsilon = \frac{\lambda - \lambda_0}{K_\varepsilon \lambda_0} \tag{2}$$

The interrogator provided the calculated strain with a gauge length of 1.28 mm and a sampling frequency of 23.8 Hz. The DOFS system was synchronized for the data capturing with the load cell.

The panel displacement along the DOFS path was computed using Ko's displacement theory. The theory relates the second derivative of the displacement y along a path x to the strain distribution divided by the panel's half thickness h (eq. 3). The theory also requires eliminating the axial strain along the fiber, which was done by measuring the strain with back-to-back SG and calculating the bending strain.

$$\frac{d^2y}{dx^2} = \frac{\epsilon(x)}{h} \tag{3}$$

On the other side, the panels of the Wagner beam were monitored through a DIC system. This system determines the full-field coordinates and displacements from digital

Figure 2. DIC measurement system with the speckled Wagner beam's panels.

images taken of the panels. A software analyzes the digital images and introduces subsets. The subsets are numerically correlated between the images resulting in measured coordinates for each subset.

This DIC system consisted of two cameras in a stereo configuration. The data was acquired with a frequency of 10 Hz. The resolution of the DIC system was optimized for the desired field-of-view by selection of lenses and standoff distances. The panel's surfaces of the Wagner beam monitored by the DIC system had a speckle pattern. The ideal speckle diameter was estimated regarding to the total camera pixel, the beam width, and the desired amount of 3-5 pixels per speckle. This resulted in a speckle size range between 0.75 mm and 1.25 mm. The DIC system positioning is illustrated in figure 2. The DIC system and DOFS were synchronized with the load cell for data acquisition.

RESULTS AND DISCUSSION

The Wagner beam mentioned above was experimentally tested and loaded under shear. The applied force and displacement of the Wagner beam were measured at the beam's load introduction point. DIC, DOFS, and SG measurements were performed up to a load of 10 kN. The campaign included 30 loading and unloading cycles.

Load-displacement behavior of all 30 trials was compared to validate the repeatability of the Wagner beam results. A close agreement was obtained with a maximum displacement scatter of 9% at 10 kN loading, excluding four outlier measurements. These trials were 15% lower in the displacement at maximum loading. This difference due to assembling/disassembling the test rig between the trials. The assembly has a major impact on the exact orientation of the load cell and LVDT and therefore caused the deviation.

Trial / Segment		DIC-side		DOFS-side			Displacement [mm]	
		SG	DIC	SG	DOFS	$DOFS_{Update}$	DIC	Clock
1	2	280	262	-550	-700	-560	2.0	2.1
	5	-515	-481	234	260	245	-2.3	-2.4
2	2	280	245	-554	-700	-558	2.0	2.1
	5	-520	-493	233	240	224	-2.3	-2.3
3	2	286	235	-562	-710	-566	2.0	2.1
	5	-528	-487	237	250	235	-2.4	-2.3
4	2	298	280	-583	-720	-570	2.1	2.2
	5	-550	-476	250	270	254	-2.4	-2.4

Table I. SG, DIC and DOFS strain measurements; DIC and clock indicator displacement measurements at the panel's center point.

Strain and displacement measurement and fiber to mid-axis distance

The table I presents strain and out-of-plane displacement measurements. The displacement measurement is conducted with a clock displacement indicator and the DIC. Both measurement methods predict similar results. The strains measured by DIC and SG are similar as well, with a maximum error less then 5%. However, discrepancies between the strain measurements from DOFS and SG arise due to their different relative position to the panel's mid-axis. SG are directly in contact with the panel's surface. The fiber for the DOFS is embedded in a layer of adhesive. Due to this adhesive, there is a small gap between the fiber and the panel's surface. To consider the gap, the distance h from the fiber to the panel's mid-axis is computed and the DOFS strain is updated in order to evaluate the strain at the panel's surface. The thickness h of segments 2 and 5 are respectively 0.67 mm and 0.52 mm. Comparing the updated DOFS strains with the SG, a close agreement is obtained.

DIC and DOFS out-of-plane displacement along the fiber path

Figure 3 shows the out-of-plane displacement along the fiber path of segments 2 and 5. For both segments measured by DIC, all 4 trials have similar curves. The panels are deflected in opposite directions. The maximum displacement at the middle peak is different between segments 2 and 5 for DIC. The maximum peak in segment 5 is -2.5mm, while in segment 2 2.1mm is achieved. The difference is caused by the manufacturing and assembly imperfection of the panel and the Wagner beam. The displacement calculated based on the DOFS measurement shows similar curves for all 4 trials except for the maximum peak. Fiber segment 2 shows a deviation of 10% between 3.2mm and 3.5mm deflection at the main peak. Fiber segment 5 shows a deviation of 20% between 1.6mm and 2mm deflection. The difference at the main peak for the DOFS is caused by the shape reconstruction method, Ko's displacement theory, because the DOFS strain distribution along both segments is similar.

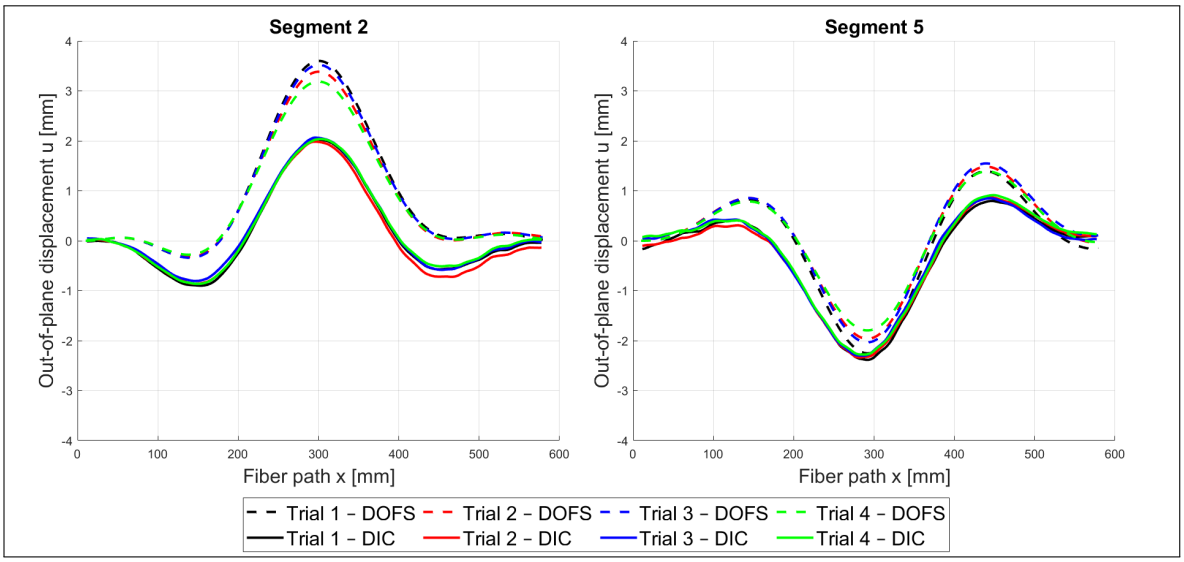

Figure 3. Out-of-plane displacement along the fiber path estimated by DIC and DOFS at 10kN load for fiber segments 2 (left) and 5 (right) for 4 trials.

Comparison of DIC and DOFS displacement

The left figure 4 shows the predicted displacement by DOFS and DIC at 10kN loading for trial 1. The DIC and DOFS are similar for segment 5 with a 5% difference at the main peak, the secondary peaks of segment 5 show a disagreement between DOFS and DIC as well. The main peaks for segment 2 show a 75% difference between DOFS and DIC. The DOFS also predicts only one secondary peak for segment 2 in contrast to the DIC. The general mismatch in the prediction of secondary peaks and the difference in the main peak for segment 2 leads to two conclusions. First, local imperfections, like fiber orientation and fiber bonding, can be the origin of peak displacement mismatch at segment 2, whilst segment 5 is satisfactorily predicted. Second, the remarkable mismatch for the secondary peaks shows that Ko's displacement theory is not suited to evaluate the full-field deformation in buckled structures strongly affected by boundary effects like panels in Wagner beam. In order to verify such behavior, the displacement calculation is repeated only for the center interval of the fiber path. These curves are shown for trial 1 in the right figure 4 which show a close agreement of DIC and DOFS displacement predictions. The differences between the peak displacement of DIC and DOFS for segment 5 is 2% and segment 2 12%. Since the difference between DIC and DOFS displacement increase moving away from the center of the plate, this conclusion is further demonstrated.

CONCLUDING REMARKS

This work compares two structural out-of-plane deformation measurement techniques. DIC was used to measure the out-of-plane deformation directly. DOFS was used to measure strain data and calculate the out-of-plane deformation based on Ko's displacement theory. The comparison was made for a Wagner beam with two aluminum alloys panels

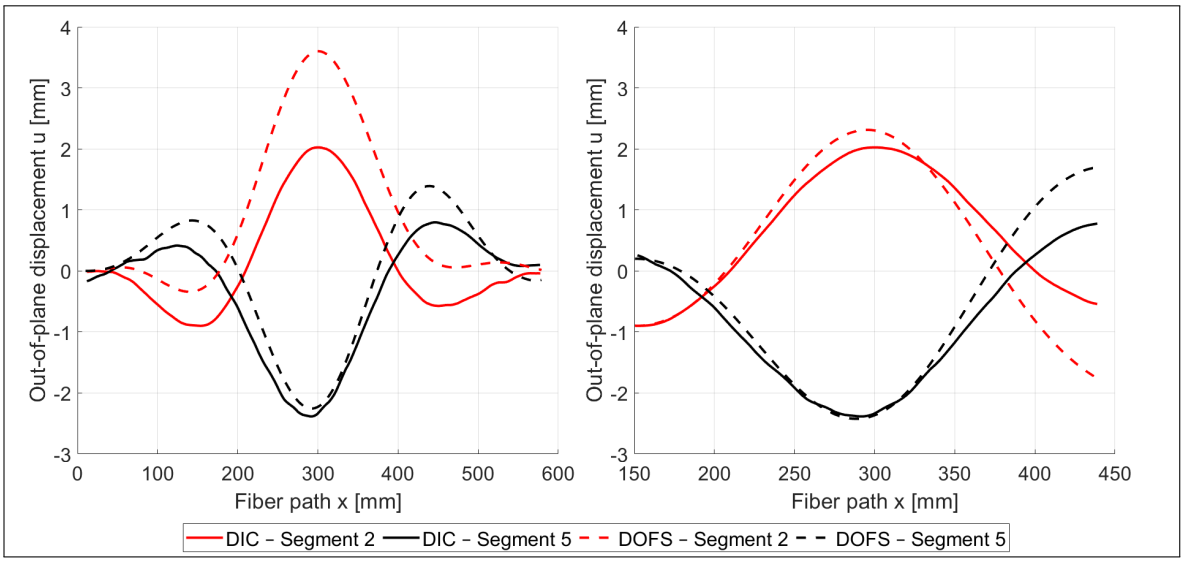

Figure 4. Out-of-plane displacement along fiber paths by DIC and DOFS at 10kN for segment 2 and 5 for Trial 1; (Left) Out-of-plane displacement for whole fiber; (Right) Out-of-plane displacement for an interval of the fiber.

shear loaded. The results of the DOFS and DIC measurements are validated by strain gauge and clock displacement measurements and the results are repeatable. The comparison between the out-of-plane displacements measured by DIC and those computed from DOFS strain data using Ko's displacement theory shows a good agreement, considering only the central area of the buckled, i.e. the plate regions unaffected by boundary effects. This demonstrates that Ko's displacement theory is suitable for describing the behavior of plates far from the boundaries. Consequently, it is necessary to further extend and refine Ko's formulation to take into account boundary effects. To improve the accuracy of the results, it is convenient to develop a more specific bonding technique that minimizes imperfections introduced during the bonding process. This result presents the first step to improve future practical health and structural deformation monitoring systems for application in light-weight and flexible aerospace structures.

ACKNOWLEDGMENT

This work was carried out within the Space It Up! project funded by the Italian Space Agency (ASI) and the Italian Ministry of University and Research (MUR) under contract No. 2024-5-E.0, CUP No. I53D24000060005.

This work is funded by the European Union (ERC Advanced Grant, NABUCCO, project number 101053309). Views and opinions expressed are however those of the author only and do not necessarily reflect those of the European Union or the European Research Council Executive Agency. Neither the European Union nor the granting authority can be held responsible for them.

REFERENCES

1. Aceti, P., L. Carminati, P. Bettini, and G. Sala. 2023. "Hygrothermal ageing of composite structures. Part 2: Mitigation techniques, detection and removal," *Composite Structures*, 319:117105.
2. Nazeer, N., G. R. M, and R. Benedictus. 2022. "Assessment of the Measurement Performance of the Multimodal Fibre Optic Shape Sensing Configuration for a Morphing Wing Section," *Sensors*, 22(6):2210.
3. Rudd, M., M. Schultz, N. Gardner, C. Kosztowny, and C. Bisagni. 2024. "Analysis and Testing of a Launch-Vehicle-Like CompositeConical–Cylindrical Shell," *AIAA Journal*, 62(9):3526–3543.
4. Pak, C. 2016. "Wing Shape Sensing from Measured Strain," *AIAA Journal*, 54(3):1064–1073.
5. Akl, W., S. Poh, and A. Baz. 2007. "Wireless and distributed sensing of the shape of morphing structures," *Sensors and Actuators A: Physical*, 140(1):94–102.
6. Foss, G. C. and E. D. Hauge. 1995. "Using modal test results to develop strain to displacement transformations," in *Proceedings of the 13th International Conference on Modal Analysis*, Nashville, TN, USA.
7. Gherlone, M., P. Cerracchio, M. Mattone, M. D. Sciuva, and A. Tessler. 2012. "Shape sensing of 3D frame structures using an inverse Finite Element Method," *International Journal of Solids and Structures*, 49:3100–3112.
8. Ko, W. L., W. L. Richards, and V. T. Tran. 2007. "Displacement Theories for In-Flight Deformed Shape Predictions of Aerospace Structures," Tech. Rep. TM-2007-214612, NASA, Edwards, CA, USA.
9. Esposito, M. and M. Gherlone. 2020. "Composite wing box deformed-shape reconstruction based on measured strains: Optimization and comparison of existing approaches," *Aerospace Science and Technology*, 99:105758.
10. Ko, W. L., V. T. Fleischer, and S. F. Lung. 2017. "Curved Displacement Transfer Functions for Geometric Nonlinear Large Deformation Structure SHape PRedictions," Tech. Rep. TM-2017-219406, NASA, Edwards, CA, USA.
11. Pak, C. 2023. "Linear and geometrically nonlinear structural shape sensing from strain data," *AIAA Journal*, 61(2):907–922.
12. Aceti, P. and G. Sala. 2024. "Impact of Moisture Absorption on Optical Fiber Sensors: New Bragg Law Formulation for Monitoring Composite Structures," *Journal of Composites Science*, 8(12), doi:10.3390/jcs8120518, all Open Access, Gold Open Access.